CAPACITIVE INTERDIGITAL SENSOR WITH INHOMOGENEOUS NEMATIC LIQUID CRYSTAL FILM

A. S. Abu-Abed and R. G. Lindquist

Electrical and Computer Engineering Department
University of Alabama in Huntsville
Huntsville, AL 35899, USA

Abstract—The performance of capacitive interdigital sensors involved with anisotropic and inhomogeneous nematic liquid crystal (LC) film is investigated. These sensors have potential applications in chemical and biological systems. The theory for modeling the permittivity tensor of the LC film as a function of the molecular orientation is presented. The LC film is handled as inhomogeneous material where molecules are assumed to have different orientations with respect to the frame axes. Under these conditions, fringing field capacitances as functions of the molecular deformations are calculated. Examples of modeled capacitive interdigital sensors in the present of different inhomogeneous distributions of LC films will be studied and discussed.

1. INTRODUCTION

Interdigital capacitors (IDC) have been involved in many sensing applications over the past five decades [1–10]. Properties of the IDC have been studied by many authors and have shown high performance when being used as sensors involved with many scientific applications. For example, interdigitated sensors are used in telecommunications, biotechnology, chemical sensing, dielectric imaging, acoustic sensors, and microelectromechanical systems (MEMS) applications [11–13].

Many features give the description of the interdigitated electrodes sensors such as sensor's geometry, mathematical modeling, manufacturing, parameter optimization, and selection of material under test. Each one of the previously mentioned applications requires certain features and parameters that achieve the goal of the application. Interdigitated sensors are well known to be combined with isotropic dielectric materials. In these cases, the sensing mechanism is based on the dielectric properties of these materials which include

physical, chemical, or structural properties of these materials. As a result, the capacitances between the electrodes forming the IDC will change.

In a previous work, the authors presented a capacitive interdigital sensors engaged with homogenous ordered LC film. An innovative technique in sensing utilizing capacitive transduction mechanism was developed and results were reported in [14]. Capacitive transduction offers significant advantages over the optical techniques adopted in [15–18]. For example, the ability to monitor the LC profile rather than simply sensing an LC distortion. Capacitive transduction also offers a simpler system for autonomous operation, greater sensitivity and potentially lower false alarms. In [14], the authors presented the theoretical and experimental principles of monitoring and tracking the nematic LC molecular profile via capacitive transduction in homogenous and ordered systems. In fact, LC films in many practical sensors are in inhomogeneous state.

This paper extends the capacitive transduction method to simulate completely inhomogeneous LC films. Molecules in nematic inhomogeneous LC films are partially disordered over all the film but can be ordered in local regions of the film. As an example, twisted nematic LC has continuous helical twist deformation which appears in layers, each layer has an average director axis where the direction of the director changes from layer to another.

2. INTERDIGITAL CAPACITOR STRUCTURE

Interdigital capacitor is a finger like or comb like periodic pattern of electrodes deposited on a broad selection of substrates which could be opaque, porous or transparent, e.g., silicon or glass, where dielectric film coats these electrodes. As shown in Figure 1, the interdigitated pattern consists of two latticed electrodes in the xy plane, each electrode consists of N fingers. Each finger has a width of a and the space between any two adjacent fingers is also set to a. The spatial distance of the periodic interdigitated cell is called a unit cell which could be defined as the distance between the centerlines of the adjacent fingers belonging to the same electrode.

By applying different potentials on the interdigitated electrodes, V_1 and V_2, the generated electric field travels from one electrode, penetrating the dielectric film, as well as the substrate underneath the electrodes, to the other electrode. The capacitance measured between the electrodes depends on the dielectric constants of the substrate and the dielectric film. Fringing capacitance between the interdigitated electrodes depends on electrode's width, a, where
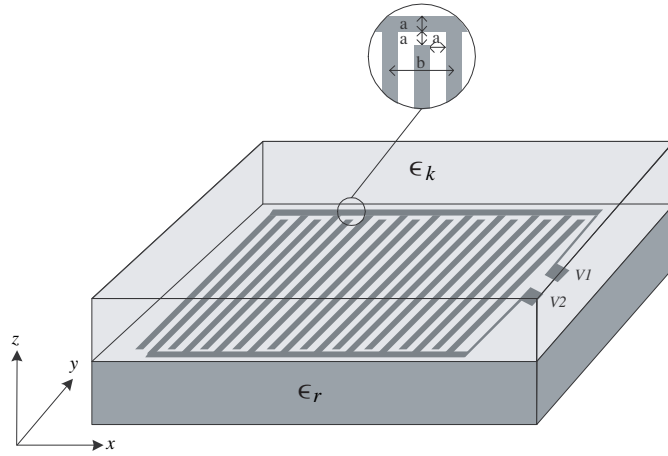
Figure 1. Interdigital capacitor (IDC).

transverse capacitance depends on the electrode's thickness, t and the distance between the adjacent electrodes. When the dielectric film is an isotropic material, the unit cell capacitance per length is given by the closed form

$$C_{uc} = \epsilon_o(\epsilon_r + \epsilon_k)\frac{K\left(\sqrt{1 - (a/b)^2}\right)}{K(a/b)} + 2\epsilon_o\epsilon_k\frac{t}{a} \qquad (1)$$

where ϵ_o is the dielectric constant in the free space, $\epsilon_o = 8.8542 \times 10^{-12}\,\mathrm{F/m}$. ϵ_r and ϵ_k are the dielectric constants of the substrate and the dielectric film, respectively. $K(\cdot)$ is the complete elliptic integral of the first kind. By making full use of symmetry and neglecting the capacitances of the edges, the total capacitance of the IDC is calculated by

$$C_{TOTAL} = C_{uc}(N - 1)L \qquad (2)$$

where N is the number of unit cells in the capacitor and L is the length of the electrode fingers.

This capacitance model is valid in the presence of an isotropic dielectric film. In the case of anisotropic film, the dielectric permittivity is a tensor rather that a single constant. In the following sections, we will numerically model the capacitance of the IDC associated with anisotropic [19–21] and inhomogeneous [22–24] LC film.

3. INHOMOGENEOUS NEMATIC LC PROFILE

Nematic LCs have anisotropic behavior below clearing temperature. LC molecules could be perfectly aligned parallel to one another or have some degree of disorder. At any point in the LC film, a vector $\vec{\mathbf{n}}$ can be defined to represent the averaged molecular orientations around that point. When the director axis is constant throughout the LC film, the film is said to be homogenous. In contrast, the LC film is inhomogeneous when the director axis changes within the film. In our analysis, we will handle different inhomogeneous molecular alignments, this requires some understanding of the molecular orientational distribution and degree of ordering of these molecules.

3.1. Molecular Orientation

Nematic uniaxial LC with rod-like (or cylinder like) has two perpendicular axes, the long axis and short axis. We will represent the molecule orientation with respect to the Cartesian coordinate system. For example, the molecule located at the coordinate points (x_i, z_j) can be described by the zenithal and azimuthal angles $\theta_{i,j} = \theta(x_i, z_j)$ and $\phi_{i,j} = \phi(x_i, z_j)$, respectively. The zenithal angle, $\theta_{i,j}$, is the angle between the long molecule axis, $\vec{\mathbf{m}}$, and the z-axis as shown in Figure 2 where the azimuthal angle, $\phi_{i,j}$, is the angle between the projection of $\vec{\mathbf{m}}$ on the xy plane and the x axis. In Figure 2, e_3 represents the long molecule axis where the short axis is represented by either e_1 or e_2, these two axes are identical due to the uniaxial nature of rod-like LC.

LC film exhibits two electrical permittivities, the parallel
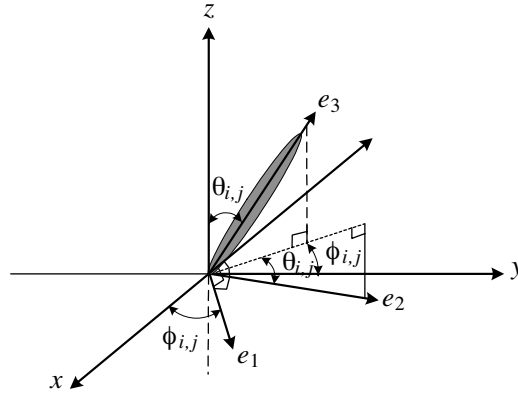
Figure 2. Geometrical representation of the rod-like molecule long axis with respect to the frame axes.

permittivity, $\epsilon_\parallel$, for the electric field traveling in parallel with the individual long molecule axis and the perpendicular permittivity, $\epsilon_\perp$, for the electric field traveling in perpendicular with the long molecule axis. The permittivity tensor, ϵ_k, in the director axis molecular principal axes system is given by

$$\epsilon_k = \begin{bmatrix} \epsilon_\perp & 0 & 0 \\ 0 & \epsilon_\perp & 0 \\ 0 & 0 & \epsilon_\parallel \end{bmatrix} \tag{3}$$

3.2. Molecular Degree of Orientational Order

In a real LC film, molecules may have certain degree of disorder. In this case, a scalar quantity is required to identify the spread of the molecules about the director axis, $\vec{n}$, and give information about the degree of order along the director axis. Let θ_r be defined as the angle between the long molecule axis and the director axis. The order parameter, which defines the degree of alignment of the molecules, depends strongly on the molecules distribution about $\vec{n}$. In general, the order parameter is defined according to the second order Legendre equation as

$$S = \frac{1}{2} \left\langle 3\cos^2 \theta_r - 1 \right\rangle \tag{4}$$

where the triangle brackets stands for the thermal average. For perfectly aligned LC film, θ_r goes to zero and the molecules have a full degree of order, i.e., $S = 1$. In contrast, when the molecules orientations are completely random, the LC film is in the isotropic phase and $S = 0$. In nematic LCs, the molecules are very sensitive to temperature and changing the temperature can cause the molecules to fluctuate and, as a result, will affect the molecular orientational distribution. Therefore, the order parameter will change as well. Moreover, the order parameter is a strongly temperature dependent parameter and can be affected by heating or cooling the LC film.

4. CAPACITANCE MODELING

We will analyze the IDC and calculate the capacitance between the electrodes numerically by using a finite difference method (FDM). applying different potentials on the electrodes will generate an electric field that satisfies Maxwell's equation

$$\nabla \cdot \left(\epsilon \vec{E} \right) = 0 \tag{5}$$

where ϵ is the dielectric permittivity and $\vec{E}$ is the electric field vector. Equation (5) can be solved for the potential V such that $\vec{E} = -\nabla V$. Since LC is anisotropic material, the dielectric permittivity, ϵ, is a tensor. According to Cartesian system, ϵ is given by

$$\epsilon = \epsilon_o \begin{bmatrix} \epsilon_{xx} & \epsilon_{xy} & \epsilon_{xz} \\ \epsilon_{yx} & \epsilon_{yy} & \epsilon_{yz} \\ \epsilon_{zx} & \epsilon_{zy} & \epsilon_{zz} \end{bmatrix} \tag{6}$$

By substituting (6) in (5), Maxwell's equation is reduced to

$$\frac{\partial}{\partial x}\left(\epsilon_{xx}\frac{\partial V}{\partial x} + \epsilon_{xz}\frac{\partial V}{\partial z}\right) + \frac{\partial}{\partial z}\left(\epsilon_{zx}\frac{\partial V}{\partial x} + \epsilon_{zz}\frac{\partial V}{\partial z}\right) = 0 \tag{7}$$

For inhomogeneous LC film, individual permittivities in (7) are functions of the space, therefore, its derivatives $\partial\epsilon_{xx}/\partial x$, $\partial\epsilon_{zz}/\partial x$, $\partial\epsilon_{zx}/\partial z$ and $\partial\epsilon_{xz}/\partial z$ are not zeros. Under this condition, (7) is ended up being

$$\left(\frac{\partial\epsilon_{xx}}{\partial x} + \frac{\partial\epsilon_{zx}}{\partial z}\right)\frac{\partial V}{\partial x} + \left(\frac{\partial\epsilon_{zz}}{\partial z} + \frac{\partial\epsilon_{xz}}{\partial x}\right)\frac{\partial V}{\partial z}$$
$$+\epsilon_{xx}\frac{\partial^2 V}{\partial x^2} + \epsilon_{xz}\frac{\partial^2 V}{\partial x\partial z} + \epsilon_{zx}\frac{\partial^2 V}{\partial z\partial x} + \epsilon_{zz}\frac{\partial^2 V}{\partial z^2} = 0 \tag{8}$$

In inhomogeneous LC film, molecules at different locations in the LC film may have different orientations. Therefore, the permittivity experienced by the electric field is different from a location to another. For example, for two different molecules located at the coordinate points (x_i, z_j) and (x_m, z_n), in general, $\epsilon_{xx}^{i,j} \neq \epsilon_{xx}^{m,n}$ when the (i,j) and (m,n) molecules have different orientations. In uniaxial rod-like LC film, the permittivity tensor is symmetrical. For example, for the (i,j) molecule, $\epsilon_{xz}^{i,j} = \epsilon_{zx}^{i,j}$, $\epsilon_{xy}^{i,j} = \epsilon_{yx}^{i,j}$, and $\epsilon_{yz}^{i,j} = \epsilon_{zy}^{i,j}$. According to the Cartesian coordinate system, the permittivity tensor for the (i,j) molecule is given by

$$\epsilon_{i,j} = \epsilon_o \begin{bmatrix} \epsilon_{xx}^{i,j} & \epsilon_{xy}^{i,j} & \epsilon_{xz}^{i,j} \\ \epsilon_{xy}^{i,j} & \epsilon_{yy}^{i,j} & \epsilon_{yz}^{i,j} \\ \epsilon_{xz}^{i,j} & \epsilon_{yz}^{i,j} & \epsilon_{zz}^{i,j} \end{bmatrix}, \tag{9}$$

where the individual permittivities in (9) are given by

$$\epsilon_{xx}^{i,j} = \epsilon_\perp + \Delta\epsilon \sin^2\theta_{i,j}\cos^2\phi_{i,j}$$
$$\epsilon_{xy}^{i,j} = \epsilon_{yx}^{i,j} = \Delta\epsilon \sin\theta_{i,j}\sin\phi_{i,j}\cos\phi_{i,j}$$

$$\epsilon_{xz}^{i,j} = \epsilon_{zx}^{i,j} = \Delta\epsilon \sin\theta_{i,j} \cos\theta_{i,j} \cos\phi_{i,j}$$

$$\epsilon_{yy}^{i,j} = \epsilon_{\perp} + \Delta\epsilon \sin^2\theta_{i,j} \sin^2\phi_{i,j}$$

$$\epsilon_{yz}^{i,j} = \epsilon_{zy}^{i,j} = \Delta\epsilon \sin\theta_{i,j} \cos\phi_{i,j} \sin\phi_{i,j}$$

$$\epsilon_{zz}^{i,j} = \epsilon_{\perp} + \Delta\epsilon \cos^2\theta_{i,j}, \tag{10}$$

Applying FDM to solve (8) inside the LC film requires dividing the film into regions, say $\Delta x \times \Delta z$. Substituting (10) in (8) and solving for the potential at (x_i, z_j) gives

$$\begin{aligned}
V_{i,j} &= (A_x + A_1)V_{i+1,j} + (A_x - A_1)V_{i-1,j} \\
&+ (A_z + A_2)V_{i,j+1} + (A_z - A_2)V_{i,j-1} \\
&+ A_{xz}(V_{i+1,j+1} - V_{i+1,j-1} - V_{i-1,j+1} + V_{i-1,j-1})
\end{aligned} \tag{11}$$

where

$$A_x = \frac{0.5\epsilon_{xx}^{i,j}(\Delta z)^2}{\epsilon_{xx}^{i,j}(\Delta z)^2 + \epsilon_{zz}^{i,j}(\Delta x)^2}$$

$$A_z = \frac{0.5\epsilon_{zz}^{i,j}(\Delta x)^2}{\epsilon_{xx}^{i,j}(\Delta z)^2 + \epsilon_{zz}^{i,j}(\Delta x)^2}$$

$$A_{xz} = \frac{0.25\epsilon_{xz}^{i,j}\,\Delta x \Delta z}{\epsilon_{xx}^{i,j}(\Delta z)^2 + \epsilon_{zz}^{i,j}(\Delta x)^2} \tag{12}$$

and

$$A_1 = A_{xz} \cdot \frac{(\epsilon_{xx}^{i+1,j} - \epsilon_{xx}^{i-1,j})(\Delta z) + (\epsilon_{xz}^{i,j+1} - \epsilon_{xz}^{i,j-1})(\Delta x)}{2\epsilon_{xz}^{i,j}(\Delta x)}$$

$$A_2 = A_{xz} \cdot \frac{(\epsilon_{zz}^{i,j+1} - \epsilon_{zz}^{i,j-1})(\Delta x) + (\epsilon_{xz}^{i+1,j} - \epsilon_{xz}^{i-1,j})(\Delta z)}{2\epsilon_{xz}^{i,j}(\Delta z)}. \tag{13}$$

Notice that for the homogenous case, $\epsilon_{xx}^{i+1,j} = \epsilon_{xx}^{i-1,j}$ and $\epsilon_{zz}^{i,j+1} = \epsilon_{zz}^{i,j-1}$, this will give $A_1 = A_2 = 0$ and Equation (11) turns into results given in [14]. The capacitance calculation requires the evaluation of $V_{i,j}$, which depends on the molecular orientation, i.e., $\theta_{i,j}$ and $\phi_{i,j}$. The capacitance per unit cell per length between any two electrodes can be calculated as follows

$$C_{uc} = \frac{\oint_{\ell} \epsilon \vec{E} \cdot d\vec{l}}{V_d} \tag{14}$$

where V_d is the potential difference between the electrodes and ϵ is the permittivity tensor of the dielectric material. It is important to notice that the potentials used to measure the capacitance in this sensor should not exceed the Freedericksz transition strength or the LC molecules will rotate as function of the potential [25].

5. RESULTS AND DISCUSSIONS

In this section, simulation results are presented to provide insight into the IDC behavior in the presence of inhomogeneous LC film. The 5CB LC parameters are used to simulate and calculate the capacitances. To get insight into the behavior of the IDC, examples of different LC alignment states will be discussed. In all these cases, we will handle IDC with interdigitated electrodes on the bottom substrate and a continuous electrode on the top one where a multilayer inhomogeneous LC film with different scenarios is sandwiched in between. In general, each layer is treated to have different average director orientation. For example, the l-th layer has an average dielectric permittivity tensor of ϵ_l, where the average director orientation is at θ_l and ϕ_l, and an order parameter of S_l, where $(l = 1, 2, 3, \ldots, L)$ and L is the number of layers. The IDC sensor with layered LC film is shown in Figure 3.
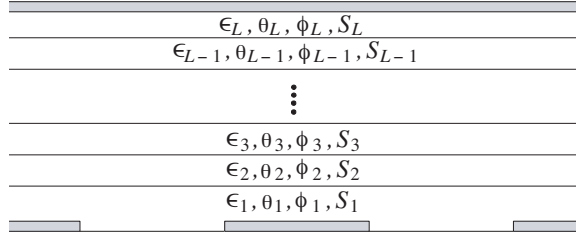
Figure 3. IDC sensor with multilayered inhomogeneous LC film.

In the first case, the molecular orientation is homogenous in each layer but inhomogeneous over all the LC films. In this structure, we consider the case of a twisted LC film in which $\theta_l = 90°$ in all layers where ϕ_l is changing from one layer to another such that ϕ_l in degrees is given by

$$\phi_l = \frac{90(l-1)}{L-1}, \qquad \text{where } l = 1, 2, \ldots, L. \qquad (15)$$

The first layer, which is near the interdigitated electrodes, has $\phi_1 = 0°$ and the last layer, which is near the continuous electrode, has $\phi_L = 90°$ as shown in Figure 4.

The permittivity tensor in each layer can be calculated by using Equations (9) and (10). When a $10\,\mu m$ thick 5CB LC film is divided into 52 layers and each layer is handled as a full ordered layer ($S_l = 1.0$, for $l = 1, 2, \ldots, L$), the fringing capacitance is $88.37\,pF$/unit cell-length compared to $91.23\,pF$/unit cell-length when the LC film is homogenous
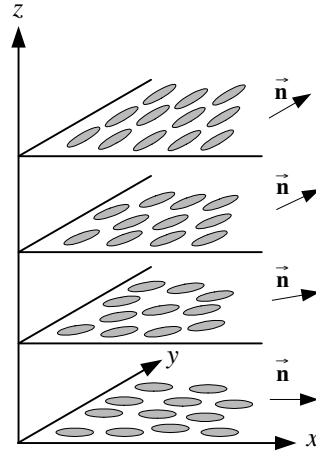
Figure 4. Multilayered twisted inhomogeneous LC film.
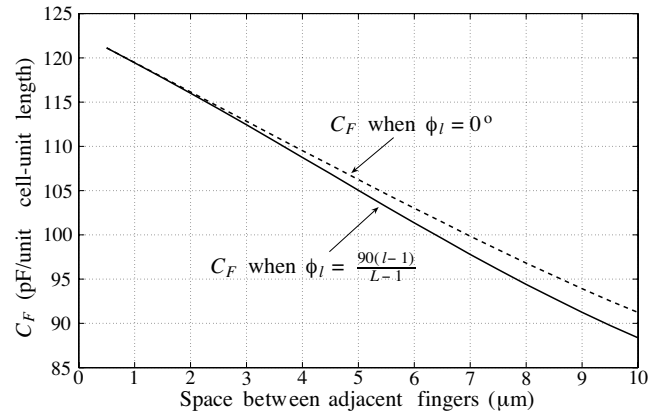
Figure 5. Capacitance, in pF/unit cell-unit length, as a function of the electrode width when $\phi_l = 0°$ and for twisted 5CB LC film.

with $\phi_l = 0$ in all layers. This shows that starting with initial homogenous alignment at $\phi_l = 0$ and stimulates the molecules to twist will result in 2.86 pF change.

In the second example, the impact of the spacing between the adjacent fingers on the capacitance is investigated. Figure 5 shows the capacitance as a function of the spacing between the adjacent fingers for both, the twisted multilayered film and when $\phi_l = 0°$ in all layers.

This example shows that the capacitances in both cases are
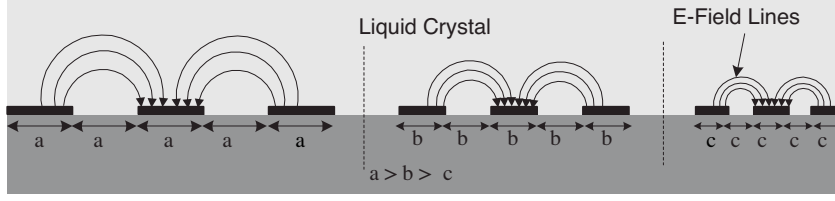
Figure 6. IDC shows penetration depth depending on the spacing between the electrodes.
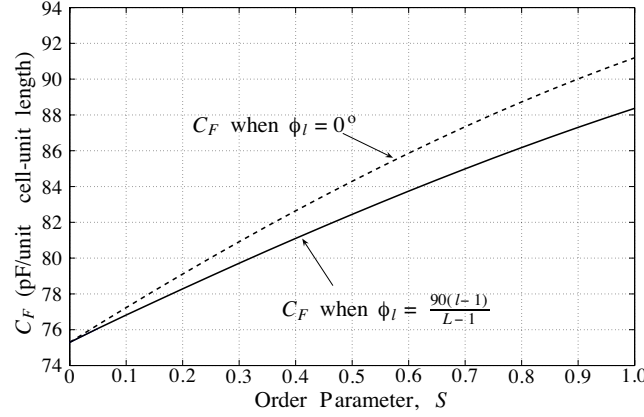
Figure 7. Capacitance, in pF/unit cell-unit length, at different order parameter values when $\phi_l = 0°$ and for twisted 5CB LC film.

very close at small spacings. The difference increases as the spacing increases. This proves that the wider the distance between the electrodes, the deeper the electric field will penetrate the LC film as shown in Figure 6. In the case of twisted director axis, the dielectric permittivity as seen by the electric field lines getting smaller as we go up the LC film. This is because molecules are parallel to the x axis in the lower layer and it is parallel to the y axis in the upper layer, thus, the electric field will see $\epsilon_\perp$ in the upper layer. On the other hand, when $\phi_l = 0$ in all layers, all the electric field lines will see molecules parallel to the x axis. This will result in capacitance difference of around 2.86 pF/unit cell/length at finger spacing of 10 μm. as shown in Figure 5.

The last example illustrate the case when molecules are partially ordered in each layer, i.e., $0 < S_l < 1$. Figure 7 shows the capacitance as a function of the order parameter in which the molecules in all layers

have the same degree of order. The solid line in Figure 7 represents the capacitance of the twisted molecules where the dashed line represents the capacitance when $\phi_l = 0°$ for all layers. When $S = 0$ for both cases, the LC film is in isotropic state and both cases have same molecular behavior and same capacitance. When $S = 1$, the results in Figure 7 are identical to those in Figure 5 when the spacing between fringing is $10\,\mu m$.

6. CONCLUSION

Interdigital capacitive sensor engaged with liquid crystal (LC) film is modeled. This partially disorder system has applications in chemical and biological sensing systems. In this paper, the LC film is handled as inhomogeneous material where each molecule, in general, has a different orientation over the region of interest. The theory for modeling the permittivity tensor of the LC film as a function of the molecular orientation was presented. IDC capacitance was modeled and impact of the LC parameters, molecules alignment, degree of ordering and spaces between the electrodes was illustrated through examples.

REFERENCES

1. Mortley, W. S., "Pulse compression by dispersive gratings on crystal quartz," *Marconi Rev.*, No. 59, 273–290, 1965.
2. Alley, G., "Interdigital capacitors and their application to lumped-element microwave integrated circuits," *IEEE Trans. Microwave Theory Tech.*, Vol. 18, 1028–1076, 1970.
3. Hobdell, J., "Optimization of interdigital capacitors," *IEEE Transactions on MTT*, 788–791, 1979.
4. Esfandiari, R., D. Maki, and M. Siracusa, "Design of interdigital capacitors and their application to GaAs monolithic filters," *IEEE Transactions on MTT*, 57–64, 1983.
5. She, X. and Y. Chow, "Interdigital microstrip capacitor as a four-port network," *IEE Proceedings, Microwaves, Antennas and Propagation*, Vol. 133, 191–197, 1986.
6. Gevorgian, S., T. Martinsson, P. Linner, and E. Kolberg, "CAD models for multilayered substrate interdigital capacitors," *IEEE Transactions on MTT*, 896–904, 1996.
7. Zhu, L. and K. Wu, "Accurate circuit model of interdigital capacitor and its application to design of new quasi-lumped

miniaturized filters with suppression of harmonic resonance," *IEEE Transactions on MTT*, 347–356, 2000.

8. Gharsallah, A., A. Gharbi, L. Desclos, and H. Baudrand, "Analysis of interdigital capacitors and quasilumped miniaturized filters using iterative method," *Int. Journal of Numerical Modeling: Electronic Networks, Devices and Fields*, Vol. 15, 169–179, 2002.

9. Niu, J.-X. and X.-L. Zhou, "Analysis of balanced composite right/left handed structure based on different dimensions of complementary split ring resonators," *Progress In Electromagnetics Research*, PIER 74, 341–351, 2007.

10. Abdalla, M. A. and Z. Hu, "On the study of left-handed coplanar waveguide coupler on ferrite substrate," *Progress In Electromagnetics Research Letters*, Vol. 1, 69–75, 2008.

11. Abbaspour-Sani, E., N. Nasirzadeh, and G. Dadashzadeh, "Two novel structures for tunable MEMS capacitor with RF applications," *Progress In Electromagnetics Research*, PIER 68, 169–183, 2007.

12. Li, L. and D. Uttamchandani, "A concept of moving dielectrophoresis electrodes based on microelectromechanical systems (MEMS) actuators," *Progress In Electromagnetics Research Letters*, Vol. 2, 89–94, 2008.

13. Mamishev, A. V., K. Sundara-Rajan, F. Yang, Y. Du, and M. Zahn, "Interdigital sensors and transducers," *IEEE Proceedings*, Vol. 92, No. 5, 808–845, 2004.

14. Abu-Abed, A., R. G. Lindquist, and W.-H. Choi, "Capacitive transduction for liquid crystal based sensors, Part I: Ordered systems," *IEEE Sensors Journal*, Vol. 7, No. 12, 1617–1624, Dec. 2007.

15. Shah, R. and N. L. Abbott, "Principles for measurement of chemical exposure based on recognition-driven anchoring transitions in liquid crystals," *Science*, Vol. 293, Issue 5533, 1296–1299, 2001.

16. Brake, J., M. Daschner, and N. L. Abbott, "Biomolecular interactions at phospholipid decorated surfaces of thermotropic liquid crystals," *Science*, Vol. 302, No. 5653, 2094–2097, 2003.

17. Shah, R. R. and N. L. Abbott, "Coupling of the orientations of liquid crystals and electrical double layers formed by the dissociation of surface-immobilized salts," *Journal of Physical Chemistry B*, Vo. 105, No. 21, 4936–4950, 2001.

18. Van Nelson, J. A., S. R. Kim, and N. L. Abbott, "Amplification of

specific binding events between biological species using lyotropic liquid crystals," *Langmuir*, Vol. 18, No. 13, 5031–5035, 2002.

19. Ding, W., L. Chen, and C.-H. Liang, "Characteristics of electromagnetic wave propagation in biaxially anisotropic left-handed materials," *Progress In Electromagnetics Research*, PIER 70, 37–42, 2007.

20. Zheng, L. G. and W. X. Zhang, "Analysis of bi-anisotropic PBG structure using plane wave expansion method," *Progress In Electromagnetics Research*, PIER 42, 233–246, 2003.

21. Wang, M. Y., J. Xu, J. Wu, B. Wei, H. L. Li, T. Xu, and D. B. Ge, "FDTD study on wave propagation in layered structures with biaxial anisotropic metamaterials," *Progress In Electromagnetics Research*, PIER 81, 253–265, 2008.

22. Rostami, A. and H. Motavali "Asymptotic iteration method: A powerful approach for analysis of inhomogeneous dielectric slab waveguides," *Progress In Electromagnetics Research B*, Vol. 4, 171–182, 2008.

23. Franceschini, G., A. Abubakar, T. M. Habashy, and A. Massa, "A comparative assessment among iterative linear solvers dealing with electromagnetic integral equations in 3D inhomogeneous anisotropic media," *Journal of Electromagnetic Waves and Applications*, Vol. 21, No. 7, 899–914, 2007.

24. Jarem, J. M., "Rigorous coupled wave theory of anisotropic, azimuthally-inhomogeneous cylindrical systems," *Progress In Electromagnetics Research*, PIER 19, 109–127, 1998.

25. Collings, P. J., *Liquid Crystals, Nature's Delicate Phase of Matter*, 2nd edition, Princeton University Press, 2002.